

Processing Techniques for Digital Sonar Images from GLORIA*

Pat S. Chavez, Jr.

National Mapping Division, U. S. Geological Survey, Flagstaff, AZ 86001

ABSTRACT: Image processing techniques have been developed to handle data from one of the newest members of the remote sensing family of digital imaging systems. This paper discusses software to process data collected by the GLORIA (Geological Long Range Inclined Asdic) sonar imaging system, designed and built by the Institute of Oceanographic Sciences (IOS) in England, to correct for both geometric and radiometric distortions that exist in the original "raw" data. Preprocessing algorithms that are GLORIA-specific include corrections for slant-range geometry, water column offset, aspect ratio distortion, changes in the ship's velocity, speckle noise, and shading problems caused by the power drop-off which occurs as a function of range.

The "cleaned-up" data base generated by the preprocessing stage can be fed as input into several information extraction and analysis routines. Spatial filters and first difference techniques were used to enhance linear type features. Pseudo sea-floor elevation data, generated entirely from the sonar image data, were used to create stereopairs and new perspective views using a portion of a sonar image. Smoothing filters combined with color coding techniques were used to identify areas with similar backscatter characteristics. The software package is part of the USGS Mini Image Processing System (MIPS) and has been used in an operational mode to process the digital GLORIA data. Two areas that have been surveyed in joint projects between the USGS and IOS are the Gulf of Mexico and the western United States coastline from Mexico to Canada for approximately 320 km offshore.

INTRODUCTION

THE USE OF DIGITAL DATA collected with remote sensing instruments has been rapidly increasing during the last two decades. One of the newest members of the remote sensing family of digital imaging systems is side-looking sonar, an active system using acoustical waves to produce images, called sonographs (Sutton, 1979). The sonographs are a measure of the reflectance properties of the sea floor's geomorphic features. Imaging sonar has many operational similarities to side-looking radar. This paper describes the computer processing techniques that have been developed to correct and enhance digital sonar images. The goal is to have the computer routines form the framework for an operational sonar processing system within the U.S. Geological Survey (USGS).

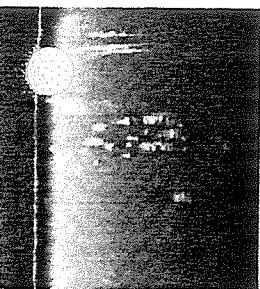
IMAGING SONAR DEVELOPMENT

During the past 5 years, the U.S. Geological Survey and the Institute of Oceanographic Sciences (IOS) from England have conducted three different sonar image collection surveys in the water bodies bordering the United States. IOS developed its first sidescan sonar in 1960 (Tucker and Stubbs, 1961),

based on earlier work reported by Chesterman *et al.* (1958). In 1965, a study was initiated to determine whether an imaging sonar system could be designed for use in the deep ocean to obtain sound images of the ocean floor (Rusby and Somers, 1977). By 1969, a sidescan sonar system called GLORIA, for Geological Long Range Inclined Asdic, was constructed and successfully tested by IOS (Rusby, 1970). The GLORIA system currently has the capability to record acoustical digital data with a 20-, 30-, or 40-second pulse-repetition rate, which produces a swath width on both port and starboard of approximately 15, 22, and 30 km, respectively, for water depths approaching 4,000 m. It has a beam pattern of 2.7° in azimuth and 10° vertically. The range requirement of 22 km for a 30-second pulse-repetition rate dictates an operating frequency of 7 KHz or less, with a 100-Hz bandwidth (Somers *et al.*, 1978).

The first USGS and IOS joint GLORIA survey took place in 1979 along a portion of the eastern coastline of the United States. The acoustical data were recorded only in analog form (Teleki *et al.*, 1981). The second joint survey occurred in early 1982 for a small area in the Gulf of Mexico; for the first time the data were collected in digital form. Many of the algorithms and computer processing techniques described in this paper to handle digital sonographs were developed, or began development, during this stage of the project. However, it was not until the third and most recent survey (April-June 1984) that

* Any use of trade names and trademarks in this publication is for identification purposes only and does not constitute endorsement by the U.S. Geological Survey.



data as it is stored on magnetic tape. The area shown is at approximately 33° north latitude, and covers an area of about 100 m by 100 m. The image is a combination of geometric and radiometric problems. The extreme edges (left and right) are distorted, and the center of the image is the nadir location.

Each line of image data contains the latitude and longitude, the nadir location for the line, the bathymetric value, the water depth offset.

For water depth also, the slant-range geometry is used. The system collects image data at a depression angle of approximately 5° to 10°. The method used to identify the across-track direction is by side-looking radar geometry (Wald and Lewis, 1976). The near-range geometry are corrected by the imaging system. The major distortion in side-looking radar systems have a depression angle difference of about 5° (much smaller). With the correction, the extreme depression angle image is less distorted. The geometry characteristics are the results of the water depth and ground-range corrections in Figure 1. Both images are stretched in order to keep the same comparison. Notice that, the near-range depression angle, the image is enlarged much more than those at mid and

far-range. The distortion present in the image is an anamorphic ratio of about 2.5. The interval in the across-track direction is 50 m. The system generates pixels with a resolution of 45 m for the across-track direction. This rate was used

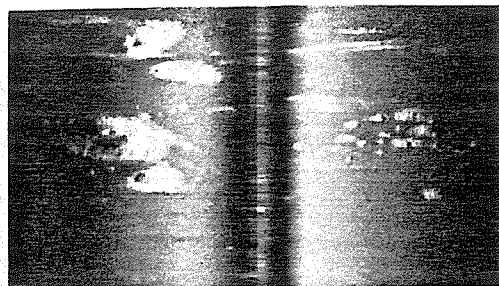


FIG. 2. This image shows the results of applying both the slant-range to ground-range and water column corrections to the image in Figure 1. Due to the extreme difference between the near- and far-range depression angles, the pixels at near-range (nadir) are expanded much more than pixels at far- or mid-range, which makes this area appear blocky. Also, pixels at nadir are now where they belong due to the water column correction.

to collect the sonar image data on the west coast. The program, which corrects for the water depth and the slant-range distortion, generates 50-m pixels in the across-track direction. However, the resolution in the along-track direction is determined by the pulse-repetition rate used (30 seconds) and the ship's velocity (7 to 10 kn). The average resolution in the along-track direction with the 30-second pulse-repetition rate is approximately 125 m, which produces images with an aspect ratio distortion of about 2.5 (that is, 125 versus 50 m).

(d) Ship Velocity Variations

Another source of geometric distortion which must be corrected is introduced by any change that occurs in the ship's velocity while it is collecting the image data. The ship's velocity can be influenced by such variables as the direction and strength of the current and/or the wind pattern with respect to the ship's direction of travel, and whether the ship is going in a straight line or is in the process of making a long turn. The velocity can often vary from 7 to 10 kn, which will cause the pixel resolution in the along-track direction to vary from approximately 110 to 140 m for a 30-second pulse-repetition rate. This introduces an "accordion" effect into the geometry of the image in the along-track direction. The distortion is removed by using the latitude and longitude extracted from the navigation data to compute the distance traveled by the ship every 30 minutes (unless a turn is detected, in which case the program uses a 10-minute interval). Given the distance traveled and the desired pixel size, it is easy to compute the number of pixels required for the particular 30-minute segment.

To simultaneously correct for the aspect-ratio distortion, a 50-m pixel size is generated on the output image in the along-track direction. This pixel size was selected so that information in the across-track direction would not be omitted due to reducing

the final pixel size or resolution (for example, 100 m instead of 50 m). In this way, the aspect ratio distortion and the distortion introduced by changes in the ship's velocity are corrected by a single program, similar to the water depth and slant-range corrections.

Figure 3 shows the results of applying these two corrections to the image shown in Figure 2. Again, the same linear contrast stretch was used to keep the contrast from product to product constant. Note that the features within the image, particularly the large volcano which is about the size of Mount St. Helens, now have more familiar geometric shapes. There are still other geometric distortions present in the image that cannot be automatically corrected (such as pointing errors), because the navigation data do not contain any pointing information, and information is generated only for pixels which are at nadir.

If maps which have acceptable resolution and geometric characteristics exist for an area, the sonar images can be geometrically registered to the maps by using control points. However, most areas (especially in the deep portions of the ocean) do not have maps of sufficient quality or resolution to allow

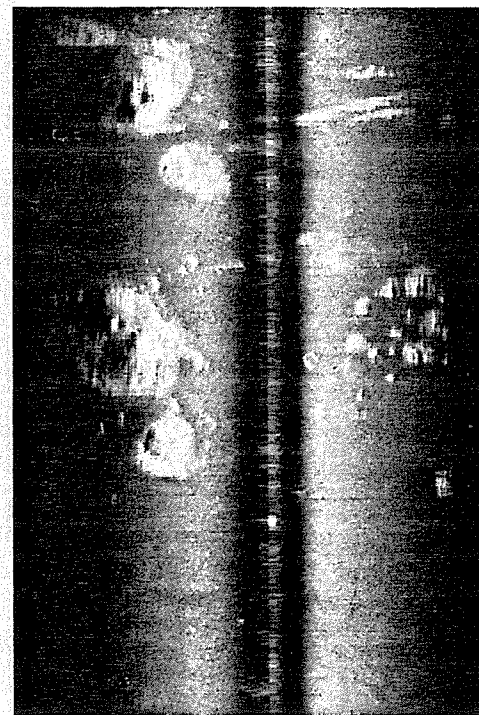


FIG. 3. This image shows the results of correcting the image in Figure 2 for both aspect-ratio distortion and ship's velocity changes in the along-track direction. Note that the features within the image, particularly the large volcanoes which are about the size of Mount St. Helens, now have more familiar geometric shapes.

the software was refined, improved, and expanded in order to create an operational/production sonar image processing system. The third survey collected data in digital form along the western United States coastline from Mexico to Canada and to approximately 320 km offshore. The survey area covered part of the newly declared U.S. Exclusive Economic Zone (EEZ). This paper describes the computer processing techniques that have been developed to correct and enhance GLORIA digital sonar images.

DIGITAL IMAGE PROCESSING REQUIREMENTS

The processing of digital data recorded by any imaging system can encompass two broad areas of computer operation — preprocessing and information extraction (Chavez *et al.*, 1977). Preprocessing techniques are designed to correct a degraded image to its intended form and are usually a precursor to information-extraction operations. Preprocessing algorithms must be customized for a particular imaging system because each has its own set of unique data-acquisition characteristics (for example, specific geometric and radiometric distortions). By contrast, information extraction techniques are more general (for example, spatial filtering, color-coding, and cover-type classification), enabling them to be applicable to data collected by any imaging system. Their goal is to improve the detectability of objects or patterns in a digital image for either visual interpretation or digital classification.

PREPROCESSING

The preprocessing applied to the GLORIA image data, as with most image data sets, is composed of three categories: (1) geometric corrections, (2) radiometric corrections, and (3) utility/miscellaneous requirements. The following discussion and examples show the various corrections used on the GLORIA sonar images and are representative of the results being generated in an operational mode within the USGS.

Geometric Corrections. Figure 1 displays the original ("raw") sonar data that are stored on magnetic tape without any corrections, incorporating only a linear contrast stretch. Several problems can easily be identified in the image. The major geometric distortions that must be corrected are caused by (a) the water column offset, (b) slant-range to ground-range projection, (c) aspect or anamorphic ratio distortion, and (d) changes in the ship's velocity.

(a) Water Column Offset

Because GLORIA starts recording data as soon as it transmits an acoustical wave, there are pixels to both sides of nadir which contain nonvalid information. In addition, the true nadir pixels (picture elements) are offset to the sides as a function of the water column or depth. Part of the GLORIA preprocessing software includes merging the appropriate navigation information from a separate file with the image data. The navigation data stored

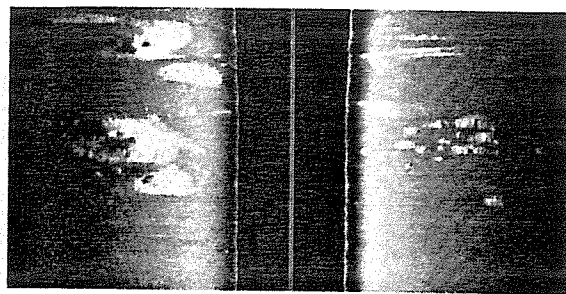


FIG. 1. Example of the "raw" data as it is stored on magnetic tape by the GLORIA imaging system. The area shown is west of southern California at approximately 33° north latitude and 123° west longitude, and covers an area of about 45 by 65 km. Various geometric and radiometric problems can be seen in the image. The extreme edges (left and right) are the far-range locations, and the center of the image is the near-range or nadir location.

in the header section of each line of image data include the time and date, latitude and longitude, and the bathymetric value at the nadir location for the given line. By use of the bathymetric value, the sonar image is corrected for the water-depth offset.

(b) Slant-Range

The program that corrects for water depth also corrects simultaneously for slant-range geometry distortions. The GLORIA system collects image data using a near-range depression angle of approximately 90°, and a far-range depression angle of 5° to 10° (Somers *et al.*, 1978). The method used to identify a pixel's location in the across-track direction is identical to the one used by side-looking radar imaging systems (MacDonald and Lewis, 1976). Therefore, images with slant-range geometry are generated by the imaging system. The major difference is that most imaging radar systems have a near- to far-range depression angle difference of at most 20° to 30° (often much smaller). With the GLORIA system, because of the extreme depression angle difference, a much more distorted image is created, but the basic geometry characteristics are identical. Figure 2 shows the results of the water depth and slant-range to ground-range corrections applied to the image shown in Figure 1. Both images incorporate the same linear stretch in order to keep the contrast constant for comparison. Notice that, due to the very large near-range depression angle, the pixels at near nadir had to be enlarged much more, by pixel duplication, than those at mid and far range.

(c) Anamorphic Distortions

Another major geometric distortion present in GLORIA images is the aspect or anamorphic ratio present between the along- and across-track directions. The sampling interval in the across-track direction is set up so that the system generates pixels which have an approximate resolution of 45 m for a 30-second pulse-repetition rate. This rate was used

this. An investigation is in progress to determine whether there is sufficient resolution in shaded-relief images made from existing bathymetric data to be used as "maps," so that a sonar image can be registered to them; however, the resolution and accuracy of the bathymetric data are questionable at this stage.

Radiometric Corrections. The second preprocessing step deals with radiometric corrections. This phase changes the digital number (DN) of a pixel rather than its spatial location, as is the case with a geometric correction. A pixel's DN value can be changed as a function of its current DN value, as a function of its position, or at times as a function of both its DN value and spatial position. The radiometric corrections needed for GLORIA sonar images include (a) shading correction due to power drop-off from near to far range, similar to radar images; a low-power problem at very near nadir due to slow power buildup by the transmitted signal; (b) speckle noise correction; and, as is the case with most scanning systems, (c) striping noise removal.

(a) Shading Correction for Power Drop-Off

The power drop-off problem is more severe in sonar images than in radar images. One reason for this is that the acoustic wave is attenuated by the hydrosphere as it travels to and from its target, whereas the microwaves used for radar imaging are not affected by the atmosphere. The power drop-off problem is very noticeable in Figure 3, as is the start-up power problem close to nadir. The method employed to correct this radiometric problem uses a two-pass algorithm. During the first pass through the data, the average value is computed for each column of the digital image in the along-track direction. This value is then normalized by the average of all the column averages, which is equal to the average of the image, to generate correction coefficients for each column that are then applied during a second pass through the data. The following equation shows the calculation needed to generate the required correction coefficients:

$$CC_i = \frac{\sum_j X_{ij}/NPTSC}{\sum_i \sum_j X_{ij}/NPTS} \quad (1)$$

where

i = column index,

j = row index,

NPTSC = total number of pixels in column,

NPTS = total number of pixels in entire image,

X_{ij} = DN value at pixel (i,j) , and

CC_i = correction coefficient for column i .

The results of using this type of shading correction are shown in Figure 4. Basically, it has the characteristics of a large spatial filter that removes large horizontal low-frequency patterns that are present due to the radiometric problems introduced by the imaging system.

Notice that, in Figure 4, most of the local details

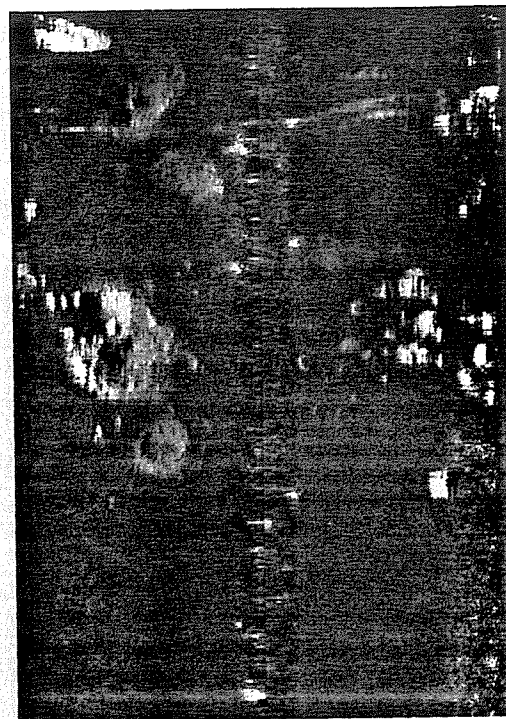


FIG. 4. This image shows the results of the shading correction which removes low-frequency brightness changes that occur in the across-track direction. The shading problem in sonar images is similar to that contained in radar images and is related to a drop-off in returned power as a function of range.

are high frequencies compared to the shading pattern seen in Figure 3. These patterns can be seen better in this image, at both the near and far range, than in the image without the shading correction. Also, by normalizing to the average of the image, rather than to a set DN value (which is an option in the software), backscatter comparisons can be made between different areas or different images. The correction also allows areas with lower or higher backscatter characteristics to be properly identified and mapped. This was not possible before the correction, because the DN values were strongly modified as a function of their range position. Profiles can now be used of different areas in the across-track direction for backscatter comparisons.

(b) Speckle Noise

Speckle noise is another radiometric problem similar to that present in radar image data (MacDonald and Lewis, 1976; Rydstrom *et al.*, 1979). It is similar to bit errors, but the contrast difference between the pixels with noise and the non-noise pixels is not as extreme. That is, the pixels which have been affected by speckle noise do not visually stand out in the image as much as pixels affected by bit errors, but their spatial frequencies are about the same. There are several methods that can be



Figure 4. The results of the shading and low-frequency brightness correction in the across-track direction. The image is similar to that shown in Figure 1, but with a drop-off in brightness at the edges.

Due to the shading pattern, the features can be seen better near and far range, than after shading correction. Also, the shape of the image, rather than the contrast difference, which is an option in the comparisons can be made for different images. The results with lower or higher contrast are not possible before the DN values were strongly affected by range position. Profiles of different areas in the across-track comparisons.

For radiometric problem in radar image data (Rydstrom *et al.*, 1979). At the contrast difference between the noise and the non-noise, that is, the pixels which have speckle noise do not visually differ much as pixels affected by low frequencies are about the same. The methods that can be

used in the spatial domain to suppress some of its effects on the visual quality of the image, especially if large-scale products are to be generated. One method developed by the author for radar image data uses a combination of a small (3 by 3 or 5 by 5) high-pass spatial filter with an appropriate threshold to identify pixels with possible speckle noise, and a small smoothing filter to remove it from the image (Chavez, 1980).

The average of the small window subtracted from the middle-pixel DN value provides information as to how much the DN differs from its neighborhood, or the window that is being used. In general, in a natural scene the DN value of a point varies by a small amount from pixels that are in a close proximity, a 3 by 3 or 5 by 5 neighborhood in this case. Changes that occur which are larger than a given limit are usually caused by something other than the natural scene characteristics in the image information, which are assumed to be valid. After the histogram of a small high-pass spatial filtered result has been visually evaluated, a threshold limit can be selected that will suppress, or set to zero, all DN values in the original image that lie outside a selected limit. Once this has been completed, low-pass filtering is executed, which acts as a smoothing filter and generates an average of a 3 by 3 or 5 by 5 window using only non-zero values. Then only the pixels having a value of zero are replaced with the average of the window. This results in the replacement of only pixels which were identified as having speckle noise, and leaves the remainder of the original data unchanged. Usually, only a small percentage of the pixels are identified as speckle noise points.

Another method that can be used for the suppression of speckle noise is by applying a small (2 by 2 or 3 by 3) smoothing filter to the entire image. This method might be preferred in cases where the speckle noise is extreme. Also, in cases as the GLORIA, it might be best to use this type of approach because it will help smooth the blocky appearance that the image will have due to the 2.5 digital enlargement that is done by pixel duplication in the along-track (line) direction due to the aspect ratio correction. Of course, one disadvantage of this method is that all data will be smoothed, instead of just a small percentage. Therefore, if the data have not been digitally enlarged by pixel duplication, the first method should be used. Figure 5 shows the results of applying a 3 by 3 smoothing filter to the image shown in Figure 4.

(c) Striping

Striping noise occurs in the across-track or scanning direction. Figure 6a shows a portion of a GLORIA sonar image with some striping noise, similar to that seen in Landsat MSS images. To remove it, a combination of high- and low-pass spatial filtering is used.

The method used to remove the striping noise is based on generating two separate images from the input data. One image represents the high-frequency

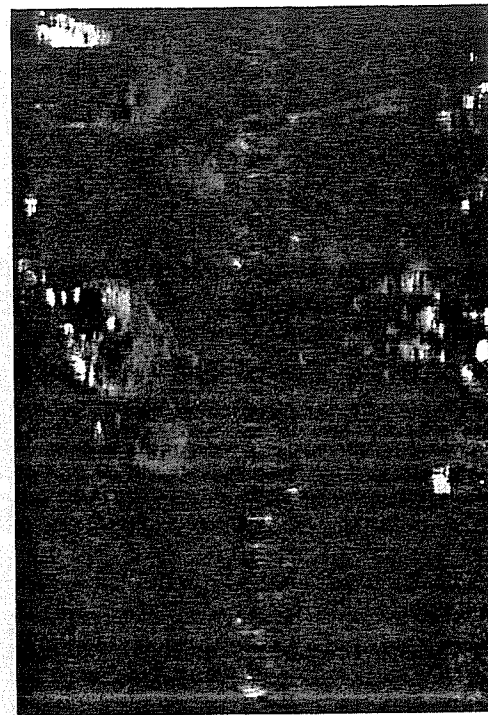


Figure 5. This image shows the results of applying a 3 by 3 smoothing filter to all the data to suppress speckle noise. A 2 by 2 filter can be used to generate a product with less smoothing.

components present in the image, except for the noise frequency; the second image represents the low-frequency components without the noise. The results of the two spatial filters are then added to create an image that is very similar to the original one, but without the noise which the convolution filters were designed to remove (Chavez and Soderblom, 1974). Let the averages of the kernels used for the high and low pass filters be represented by AVEH and AVEL, respectively. If the DN value of the pixel or point at the center of each of the two kernels is represented by PTXH and PTXL, high and low pass respectively, then the following can be used to generate the high and low frequency components needed:

$$\begin{aligned} \text{HFC} &= \text{PTXH} - \text{AVEH} \\ \text{LFC} &= \text{PTXL} \end{aligned} \quad (2)$$

The final results can then be generated as follows:

$$\text{RESULTS} = \text{HFC} + \text{LFC} \quad (3)$$

The filter shapes used to remove the striping noise from the GLORIA sonar images were a 1 line by 71 sample high-pass filter, and a 21 line by 71 sample low-pass filter. For comparison, the shapes of the filters needed to remove the striping in Landsat MSS images are a 1 line by 101 sample high-pass filter, and a 7 line by 101 sample low-pass filter. Figure 6b

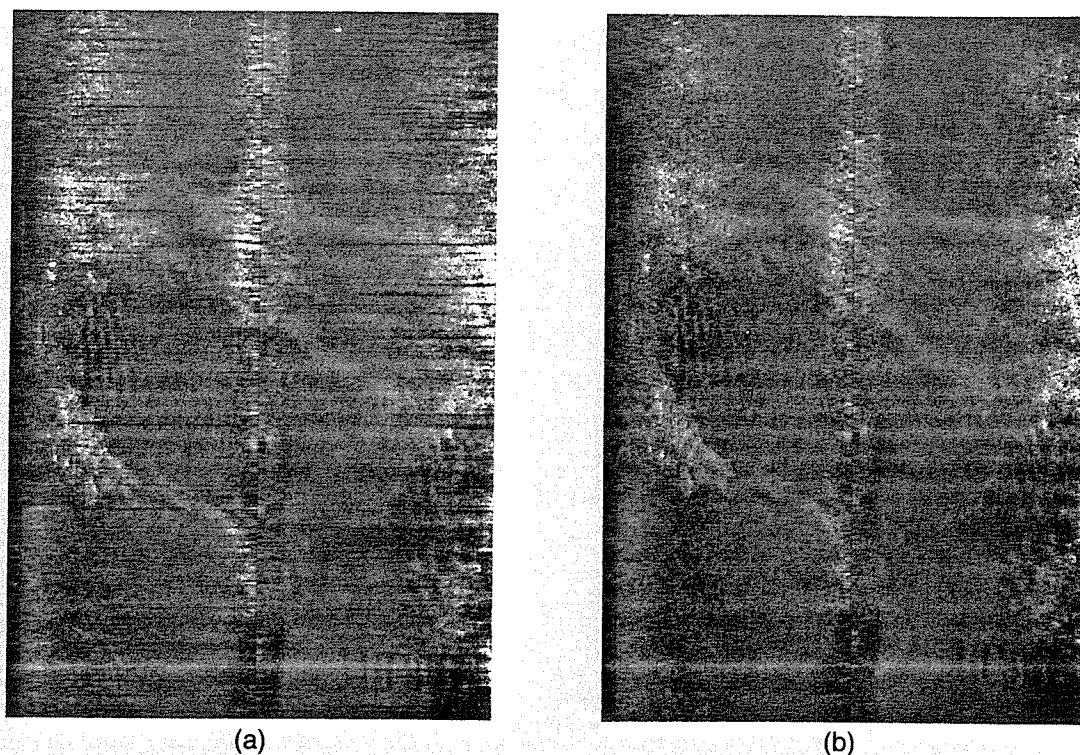


Fig. 6. (a) This image shows an example of the striping problem that is in the GLORIA data, similar to that often seen in most scanning imaging systems. (b) This image shows the results of striping noise removal using convolution filtering techniques applied in image space. Note that only the striping frequency has been removed.

shows the results of the striping noise removal applied to the image shown in Figure 6a. This method is applicable to other noise patterns as well, the only difference being that the shape of the spatial filters must be designed for the particular noise pattern to be removed.

Utility/Miscellaneous Requirements. In most cases there are a few miscellaneous techniques that can be used as tools, either to further improve the analysis of the final product or to examine the results of the various preprocessing steps. Several such tools were used with the GLORIA data. One utility allows profiles of data stored on disk to be drawn on the system's T.V. display screen. Profiles of data in the across-track direction of each preprocessing result provide an alternate means of seeing what each geometric and/or radiometric correction has done to the data. For example, a profile of all the following can be drawn on the screen with different colors assigned to each profile: original image, water depth and slant-range corrections, aspect ratio and delta velocity corrections, and shading correction.

Another utility that has proven very valuable in the film mosaicking stage is the generation of a T-bar, which points approximately north on the left side of the image. A T-bar is placed every 500 lines and does not point exactly north because a 32 by 32

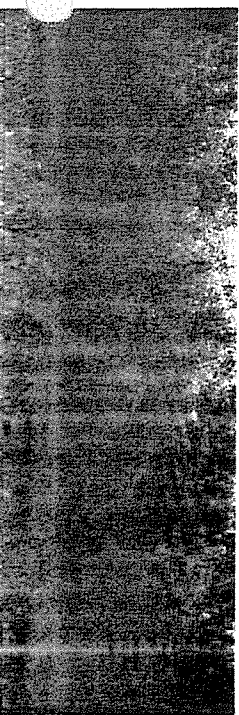
pixel array is used, which can have a pointing error of plus and minus 3° . However, this accuracy is more than adequate for its intended use.

INFORMATION EXTRACTION

The preprocessing requirements are related very specifically to the imaging system being used, and are applicable regardless of the intended use of the data (for example, vegetation or geologic mapping). The final results of the preprocessing phase become the "cleaned-up" data base that is then used as input for information extraction and analysis techniques. It is at this stage that the types of algorithms and methods used to analyze and extract information from the image data become dependent on the user's special interest.

There are many different methods to analyze and extract useful information from an image. Two categories of techniques that have been found useful with the GLORIA data are (1) enhance/extract structural information (i.e., high-pass spatial filtering and perspective views of the data) and (2) map areas with similar backscatter characteristics (that is, spatial filtering combined with color coding).

Structural Enhancement. A major interest of GLORIA data users is the enhancement of linear features,



data, similar to that often
removal using convolution
on removed.

can have a pointing error
however, this accuracy is
intended use.

rements are related very
system being used, and
of the intended use of the
on or geologic mapping).
processing phase become
that is then used as input
and analysis techniques.
types of algorithms and
and extract information
dependent on the user's

methods to analyze and
from an image. Two
t have been found useful
re (1) enhance/extract
high-pass spatial filtering
e data) and (2) map areas
characteristics (that is, spatial
or coding).

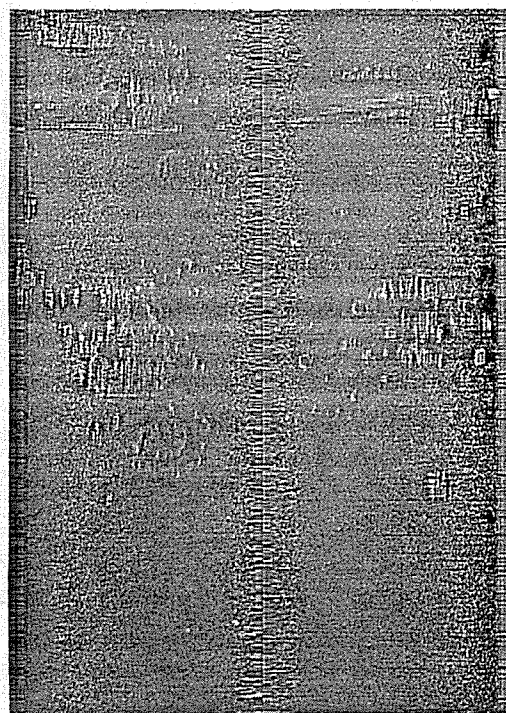
major interest of GLORIA
ment of linear features,

including seamount chains, mountains, possible joints and faults, and underwater channels. The spatial-filter program used by the USGS in Flagstaff has many different options, which include high-pass spatial filtering that enhances linear features (Chavez *et al.* 1976; Seidman, 1972). The program applies a Laplacian type filter, and can have a kernel size of M by N pixels. The values for M and N can range from 1 to 501, and M can be equal or unequal to N . Processing time is independent of the filter size after the initial few seconds needed to compute the starting sums.

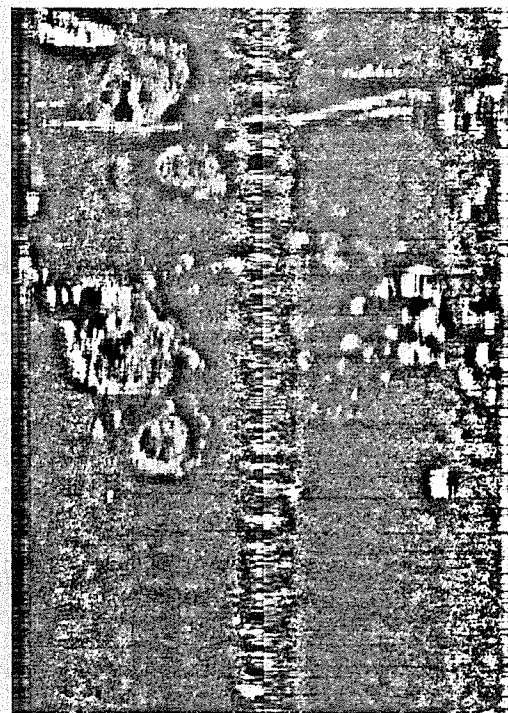
The size of the filter is dependent on the size of linear features the user is interested in enhancing. In general, as filter size decreases, the smaller the detail it will enhance and vice versa. For image data with 50- and 100-m spatial resolution, filter sizes that often generate useful products range from 11×11 to 101×101 pixels. Figures 7a and 7b show the results of applying two different high-pass spatial filters to the image shown in Figure 4. Notice the enhancement of the local detail in both dark and bright areas. This type of processing helps to visually identify and map linear features throughout the entire image.

If the user is interested in linear features that are at the spatial resolution limits of the imaging system, a first difference (which approximates the first derivative of the image) can be generated in the horizontal, vertical, or diagonal direction of the image (Chavez *et al.* 1976). This technique removes most frequencies except those close to the resolution limits of the system. Usually the information removed includes backscatter characteristics, or albedo in the case of Landsat MSS images, of all cover types. This is also the case, but to a lesser degree, with high-pass spatial filtering. In data such as in GLORIA sonar images, the first difference can be strongly affected by the signal-to-noise level, and the resultant image will appear very busy. This effect can be seen in Figure 8a, which represents the first difference results of the image shown in Figure 4. Note that, due to the busy nature of the image, some of the linear features are not easily seen.

A technique that can be used to improve the visual appearance of a first difference image is the application of a linear contrast stretch coupled with a small smoothing spatial filter. The linear contrast stretch is applied first, to spread the DN range over most of the 0 to 255 range that is available. This is



(a)



(b)

FIG. 7. (a) This image shows the results of applying an 11 by 11 high-pass spatial filter to the image in Figure 4. The data had a linear stretch applied after filtering to increase the contrast. (b) This image shows the results of applying a 61 by 61 high-pass spatial filter to the image in Figure 4. The data had a linear stretch applied after the filter to increase the contrast. Notice that the larger the filter size, the larger the features, or the lower the frequencies, that are enhanced.

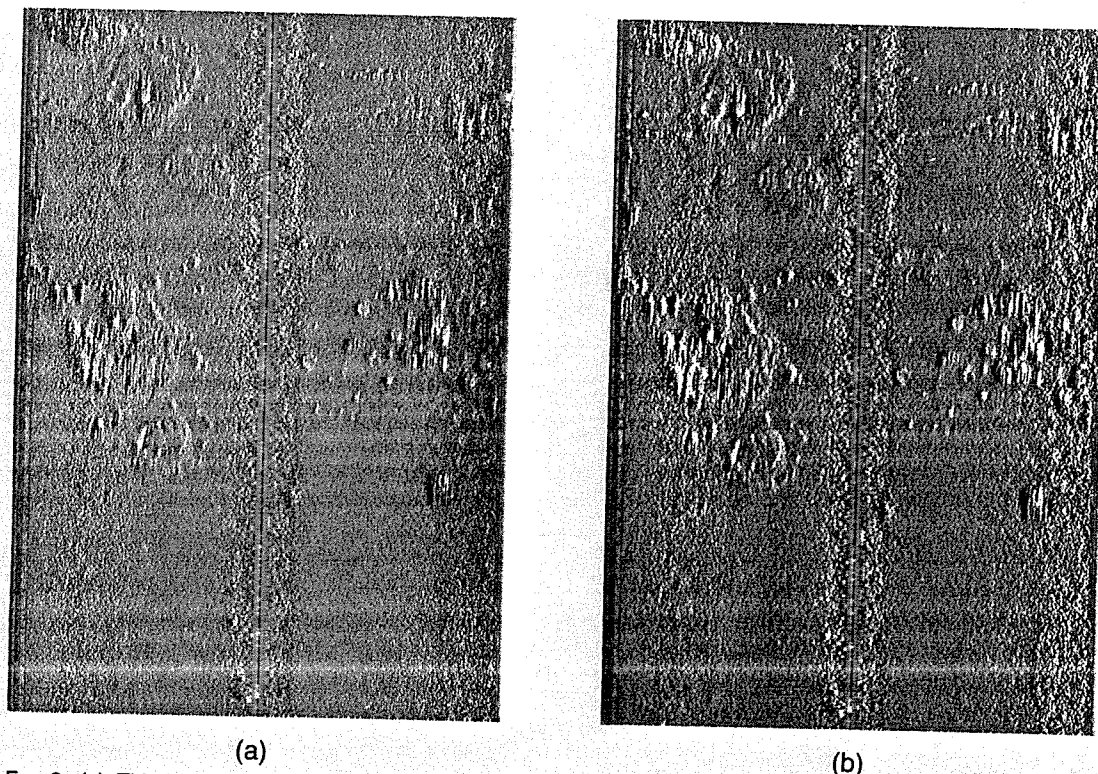


FIG. 8. (a) This image shows the results of the horizontal first difference of the image in Figure 4. It has had a linear stretch applied to increase the contrast. Note how busy the image is due to the signal-to-noise ratio of the data. (b) This image shows the results of applying a small smoothing filter (3 by 3) to the first difference image shown in Figure 8a. The data had a stretch applied before the smoothing filter in order to create "holes" or voids in the DN range. This increased the number of DN values that were available during the filtering process.

done because the first difference image usually has a very narrow DN range (for example, 110 to 144). By stretching the DN values over most of the 0 to 255 range before applying a small smoothing spatial filter, "holes" or voids are created between the DN values that are in the first difference image. This will give the smoothing filter "extra" DN resolution. Without these "holes," the smoothing filter would map different DN values together, especially if the majority of the pixels in the filter kernel are made up of the background DN value (127), and the pixel being processed has a DN value near that. Figure 8b shows the results of applying a linear contrast stretch and a small smoothing filter to the first difference image shown in Figure 8a.

Another method that can be used to enhance linear features is to either generate a stereopair or create an image with a new perspective view. Usually a hydrography/elevation model or "image" is required to create either one of these two products. However, when using only a small image, areas can be found where the majority of the DN values representing brightness or sonar backscatter is being modulated by the geometry or slope of the topography.

Furthermore, a high-pass spatial filter can be applied to the image, if needed, which will decrease the influence of the cover types on the backscatter modulation and make the resultant image even more dependent on slope and topography. With this in mind, and on an experimental basis, stereopairs and new perspective views of some of the GLORIA image data have been created with encouraging results using the recorded DN values.

Figure 9 is a stereogram generated by using the processed GLORIA image data (shown in Figure 4) as input. In general, the topographic highs and lows are shown as expected, but further work is still needed, and an algorithm to integrate the DN values is required to create an elevation model. As it is currently programmed, the method sees shadows on the back side of mountains as low areas, and depressions or holes are created in these areas. Research is being conducted for the development of an acceptable algorithm to create a "better" digital elevation model from the sonar image data.

By using the GLORIA image data as above, a new image with a different perspective view can also be generated. The viewer can be placed at any elevation,

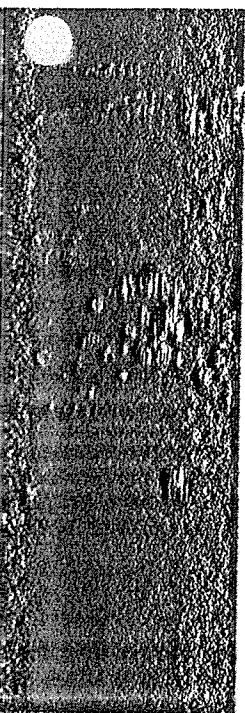


Figure 4. It has had a signal-to-noise ratio of the first difference image created "holes" or voids in the process.

spatial filter can be applied which will decrease the noise on the backscatter resultant image even more topography. With this in mind, stereopairs and some of the GLORIA image with encouraging results.

generated by using the data (shown in Figure 4) topographic highs and lows but further work is still needed to integrate the DN values into a elevation model. As it is, the method sees shadows and treats them as low areas, and not as high areas. This is a problem for the development of a "better" digital sonar image data.

As above, a new perspective view can also be created at any elevation,

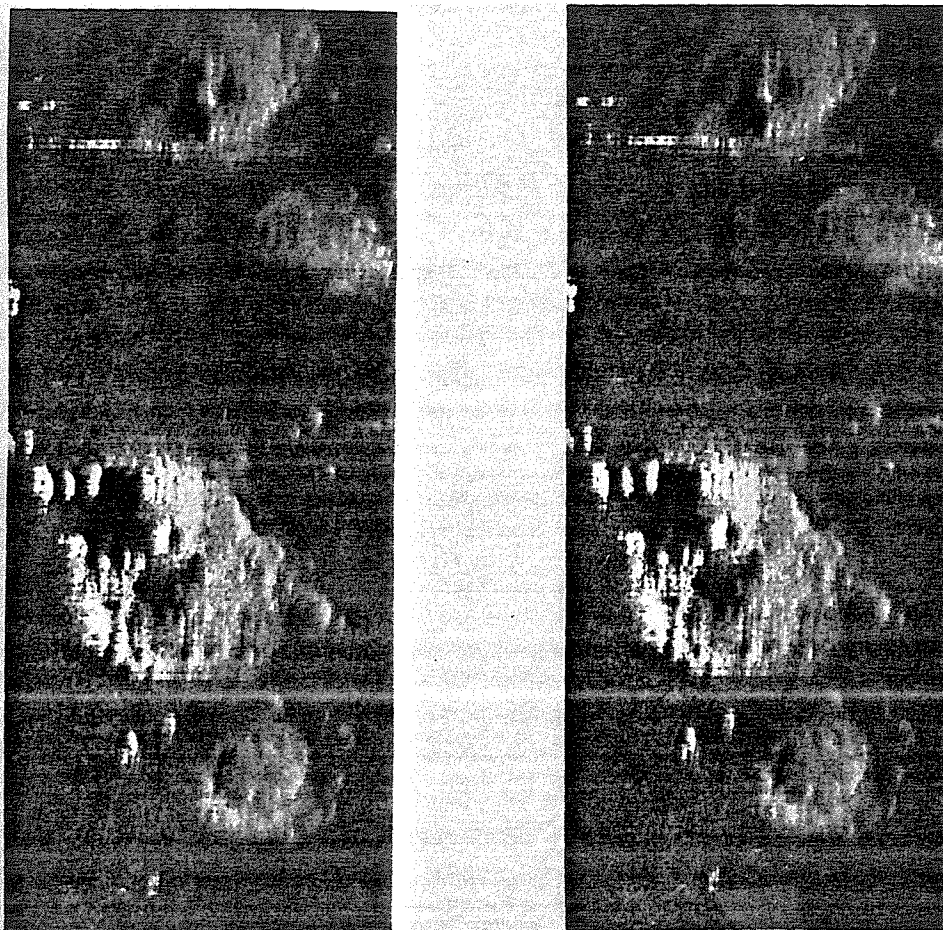


FIG. 9. These two images form a stereopair created solely from the image data. The image on the left is the image shown in Figure 4 with parallax introduced as a function of "sonar brightness." The image on the right is the same image shown in Figure 4 and is the original data.

viewing from any direction, to create an image which appears to have been recorded from that location. Figures 10a and 10b represent two such new perspective views of the image in Figure 10a. The new viewing angles are 45° and 70° from vertical, respectively. Problems related to the "non-real" hydrography image used to create these products can be seen, but the products are still useful in the analysis stage, as long as the user keeps in mind the method by which they were created.

Backscatter Mapping. As with linear feature enhancement, there are many different methods that can be used to enhance or map similar brightness or backscatter areas. However, using a data base that has only a monochromatic image, as opposed to one with multispectral images like the Landsat MSS, reduces the number of methods that can be used. One obvious method is to use a linear contrast stretched image and do simple photo interpretation.

A method that can be used interactively is to apply density slicing to the 8-bit monochromatic image in the digital domain. However, because the human eye can see color differences more easily than tonal differences (and more of them), it is better to apply color coding techniques.

There are several ways to assign colors to an 8-bit black-and-white image using either interactive or fully automatic methods. The examples shown here were generated using a fully automatic method, the brightness ranges selected being based on equal DN and equal percent color assignments. The equal DN color coding method will preferentially enhance the ends of the frequency histogram the most, while the equal percent, which is equivalent to histogram equalization, will enhance the middle part of the frequency histogram the most. However, before color coding data like the GLORIA sonar images, better results can be generated if a small amount of spatial

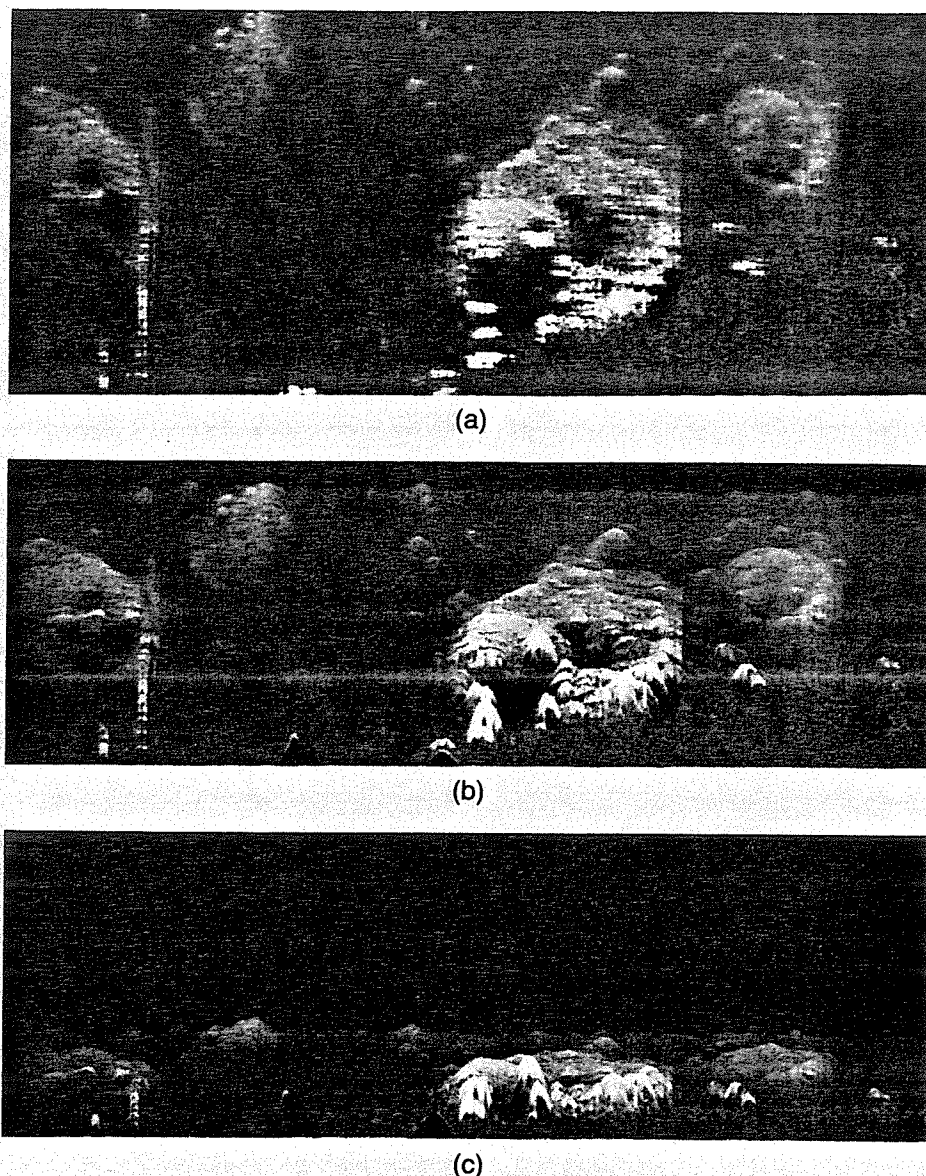


FIG. 10. Top image (a) is a portion of the image shown in Figure 4. Using the same pseudo-hydrographic file created to generate the stereopair in Figure 9, new perspective views can be created. The middle image (b) and bottom image (c) show two such new perspective views with viewing angles of 45° and 70° from vertical, respectively.

smoothing is applied first (this is also true of water enhancement using Landsat MSS). This helps reduce the effects of random noise and/or isolated pixels, and creates an image with much more homogeneous patterns. Plate 1 shows the results of equal percent color coding applied to the GLORIA data without using a smoothing filter. Plate 2 shows the results when the same color coding has been applied to the data after smoothing. For comparison, Plate 3 shows the smoothed data color coded using an equal DN color coding method.

Another method can be used to color code monochromatic images to generate a continuous color spectrum instead of a quantized/sliced spectrum. The data must be contrast stretched with three different stretches and a color composite made. An example of this type of color coding is shown in Plate 4, where the data were stretched so that high DN values were mapped to red, middle DN values to green, and low DN values to blue. The graph in Figure 11 shows the contrast stretches used to generate this product. Other products could easily be generated



same pseudo-
views can be
active views with

used to color code
generate a continuous color
sliced/sliced spectrum. The
with three different
site made. An example
is shown in Plate 4,
so that high DN values
DN values to green,
The graph in Figure 11
used to generate this
could easily be generated

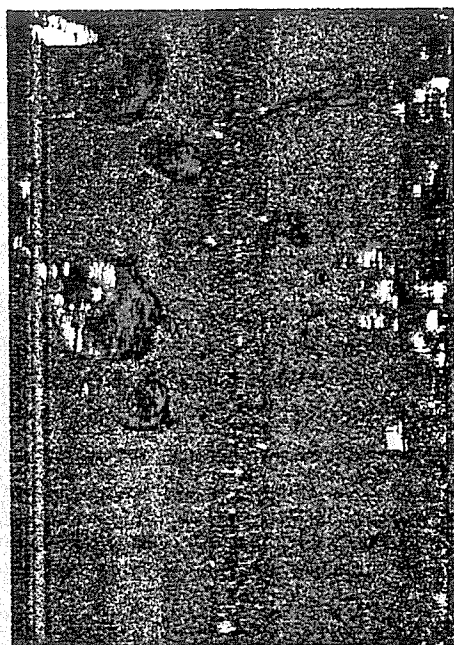


PLATE 1. This image shows the results of applying color coding to the image in Figure 4. The color coding method used was equal percent, which is similar to histogram equalization, with no smoothing applied prior to color assignments. Notice that the image is quite busy and that most patterns are not very clear.



PLATE 3. This image shows the results of using an equal DN color coding technique instead of equal percent as shown in Plate 2. This enhances the ends of the DN distribution more than the middle range. Notice the added detail within the dark and bright regions of the large volcano, but the loss of detail in areas with mid-DN values.

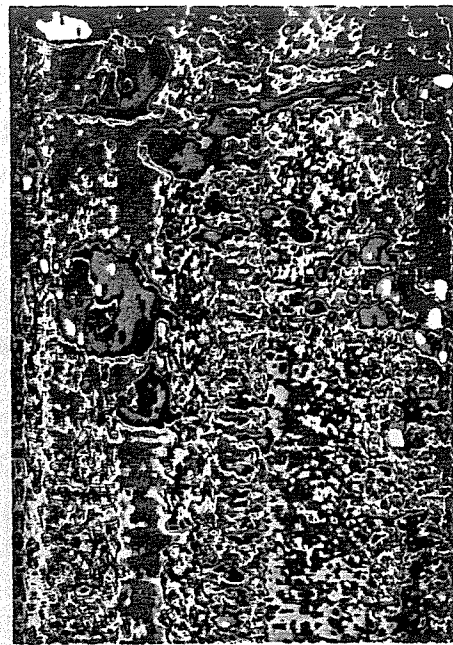


PLATE 2. This image was color coded with the identical parameters used for Plate 1, but after smoothing had been applied to the input image. Notice that patterns are seen much easier in this image than in Plate 1, and are more like those seen on maps made by photointerpreters. Equal percent color coding, used to generate this product, enhances the mid-DN range of a histogram more than the ends.

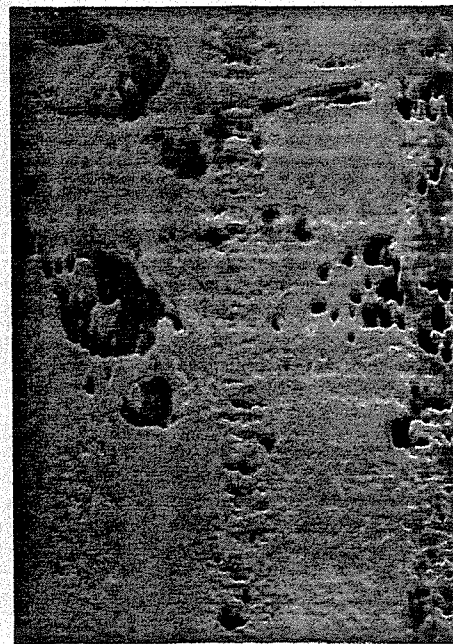


PLATE 4. This image shows an example of color coding the data so that a continuous spectrum is generated. The methods used in Plates 2 and 3 generate quantized color changes. The color boundaries can change radically depending on how the data is "sliced." The image shown here was color coded so that high DN values are red, mid-DN values are green, and low DN values are blue. Figure 11 shows a graphic representation of the method used to generate this product.

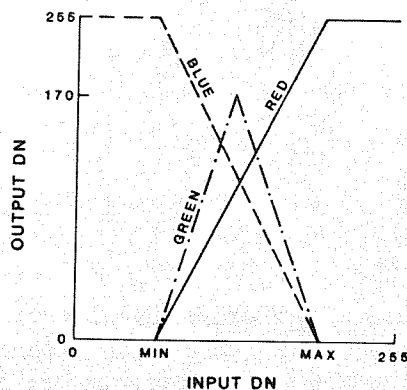


FIG. 11. Graphic representation of the linear (blue and red) and piece-wise linear (screen) stretches that can be used to generate a color composite of a monochromatic image so that it will have a continuous color spectrum. In this example, the high DN values are mapped red; mid-DN values, green; and low DN values, blue. This combination was used to generate the image shown in Plate 4 with MIN and MAX values of 20 and 125, respectively. Variations of this product can be generated by changing the relationship of the stretches (for example, harder stretch on the red and softer stretch on the blue; or by using a ramp/multipiece-wise function in one of the colors).

by using different stretch patterns (for example, reduce the blue and green range, and increase the red component range).

SUMMARY

Software has been designed, written, and expanded during the past 4 years to process digital images from the GLORIA system. The USGS and IOS have had three joint projects to survey areas near the United States, and other surveys are planned. The software to process the sonar images is separated into the two categories of (1) preprocessing and (2) analysis and information extraction.

The various products being generated show, often for the first time, detailed information that will be used to map the ocean floor. These maps will give the large overview "picture" of the region, similar to regional views of land areas provided by Landsat MSS images, and will help identify areas of interest for further detailed studies for exploration and/or potential hazard areas. The software to process the GLORIA data is part of the USGS MIPS developed in Flagstaff and duplicated in USGS offices in Menlo Park, California, and Reston, Virginia (Chavez, 1984).

Current GLORIA-related research involves converting the bathymetric and magnetic data, collected for nadir locations every 2 minutes, from vector to raster format and generating surfaces covering 2°

by 2°. These surfaces will be registered to digital mosaics of the sonar data for analysis and information extraction. Work will also continue on extracting hydrographic information from the sonar images, as well as registering the sonar images to a shaded-relief base.

ACKNOWLEDGMENTS

The author would like to acknowledge Paul Teleki for having introduced him into sonar image processing, and for being the driving force within the USGS for using the GLORIA system in the first two surveys. Jim Gardner was responsible for the most recent, and largest, survey in the west coast. Because this survey covered such a large area and because of the interest caused by the implementation of the EEZ, the software was made into an operational package to create image maps. The author would also like to thank Mike Somers from IOS whose discussions, especially about slant-range geometry corrections, throughout the three joint surveys proved to be very valuable. Also, during the recent survey Jeff Anderson helped with the software to merge the navigation and image data, as well as converting the image data into the proper format.

REFERENCES

- Chavez, P. S. Jr., 1980. *Automatic shading correction and speckle noise mapping/removal techniques for radar image data*. National Aeronautics and Space Administration, JPL Publication 80-61, pp. 251-262.
- 1984. *U.S. Geological Survey mini image processing system (MIPS)*. U.S. Geological Survey Open-File Report 84-880, 12 p.
- Chavez, P. S., Jr., G. L. Berlin, and A. V. Acosta, 1976. Computer processing of landsat MSS digital data for linear enhancements. *Proceedings of 2nd W. T. Pecora Memorial Symp.*, Sioux Falls, S.D., pp. 235-250.
- Chavez, P. S., Jr., G. L. Berlin, and W. B. Mitchell, 1977. Computer enhancement techniques of landsat MSS digital images for land use/land cover assessments. *Sixth Remote Sensing of Earth Resources Symposium*, Tulsa, TN., March 1977, pp. 259-275.
- Chavez, P. S., Jr., and L. A. Soderblom, 1974. Simple high-speed digital image processing to remove quasi-coherent noise patterns. *American Society of Photogrammetry Symposium*, Washington, D.C., pp. 595-600.
- Chesterman, W. D., P. R. Clynick, and A. H. Stride, 1958. An acoustic aid to sea-bed survey. *Acoustica*, Vol. 8, pp. 285-290.
- MacDonald, H. C., and A. J. Lewis, 1976. Operation and characteristics of imaging radar systems. *Journal of Remote Sensing of the Electro Magnetic Spectrum*, July, Vol. 3, No. 3, pp. 23-45.
- Rusby, J. S. M., 1970. A long range side-scan sonar for use in the deep sea (GLORIA project). *International Hydrographic Review*, Vol. 47, pp. 25-39.
- Rusby, J. S. M., and M. L. Somers, 1977. The development of the GLORIA sonar system from 1970 to 1975. In M. V. Angel, (ed.), *Voyage of Discovery*, suppl. to *Deep Sea Research*, Vol. 24, pp. 611-625.

be registered to digital for analysis and information to continue on information from the sonar images to a

CONCLUSIONS

We acknowledge Paul Teleki for his contribution into sonar image processing and the driving force within the GLORIA system in the first survey. He was responsible for the survey in the west coast. He had such a large area and was assisted by the implementation of the software. The author would like to thank the Somers from IOS whose contribution to slant-range geometry in the three joint surveys. Also, during the recent survey, the software was updated with the software to process image data, as well as to convert the data into the proper format.

REFERENCES

Teleki, P. G., 1979. Shading correction and speckle reduction techniques for radar image data. *Proceedings of IEEE*, Space Administration, JPL, pp. 255-262.

Teleki, P. G., 1981. Image processing system for the GLORIA Open-File Report.

Teleki, P. G., and A. V. Acosta, 1976. Landsat MSS digital data for the GLORIA project. *Proceedings of 2nd W. T. Pecora Conference*, S.D., pp. 235-250.

Teleki, P. G., and W. B. Mitchell, 1977. Techniques of Landsat MSS data for land cover assessments. *Resources Symposium*, Tulsa, pp. 259-275.

Teleki, P. G., and E. L. Blom, 1974. Simple high-resolution technique to remove quasi-coherent artifacts. *International Society of Photogrammetry and Remote Sensing*, D.C., pp. 595-600.

Teleki, P. G., and A. H. Stride, 1958. Sonar survey. *Acoustica*, Vol. 8, pp. 1-10.

Teleki, P. G., 1976. Operation and maintenance of sonar systems. *Journal of Remote Sensing*, July, Vol. 10, pp. 1-10.

Teleki, P. G., 1977. The development of sonar systems from 1970 to 1975. In *M. J. R. Canty, ed., Deep Sea Research*, Vol. 24, pp. 1-10.

Teleki, P. G., 1977. The development of sonar systems from 1970 to 1975. In *M. J. R. Canty, ed., Deep Sea Research*, Vol. 24, pp. 1-10.

Rydstrom, H. O., G. L. La Prade, and E. S. Leonardo, 1979. *Radar imagery interpretation adaptable to planetary investigations*. Goodyear Aerospace Corp., Arizona Division, Goodyear, Arizona, 228 p.

Seidman, J. B., 1972. Some practical applications of digital filtering in image processing. *Proceedings of Computer Image Processing and Recognition Symposium*, University of Missouri, Columbia, Missouri, August 1972.

Somers, M. L., R. M. Carson, J. A. Revie, R. H. Edge, B. J. Barrow, and A. G. Andrews, 1978. GLORIA II—an improved long range sidescan sonar. *Proceedings of IEEE/IERE Subconf. on Ocean Instruments and Communication; Oceanology International*, B.P.S. Pub. Ltd., London, pp. 16-24.

Sutton, J. L., 1979. Underwater acoustic imaging. *Proceedings of IEEE*, April 1979, Vol. 67, No. 4, pp. 554-566.

Teleki, P. G., D. G. Roberts, P. S. Chavez, M. L. Somers, and D. C. Twichell, 1981. Sonar survey of the U.S. Atlantic continental slope; acoustic characteristics and image processing techniques. *Proceedings of 13th Annual Offshore Technology Conference*, May, 1981, Houston, Texas, pp. 91-102.

Tucker, M. J., and A. R. Stubbs, 1961. A narrow beam echo-ranger for fishery and geological investigations. *British Journal of Applied Physics*, Vol. 12, pp. 103-110.

(Received 13 August 1985; revised and accepted 21 February 1986)

CALL FOR PAPERS 1987 ISPRS Intercommission III/IV Symposium Digital Technology for the Integration of Photogrammetric and Remote Sensing Data with Land/Geographic Information Systems

April 1 - 2, 1987
Baltimore, Maryland

This Symposium is being sponsored by the International Society for Photogrammetry and Remote Sensing (ISPRS) and will be held in conjunction with the 1987 ASPRS/ACSM Annual Convention (March 29 - April 3) and the AUTO CARTO 8 International Symposium on Automation in Cartography (March 30 - April 2). The program will include invited and presented papers on the following subjects:

- Interface Between Photogrammetry/Remote Sensing and Digital Image Processing/Computer Graphics
- Geocoded Data Bases, Land Information Systems (LIS) and Geographic Information Systems (GIS)
- Digital Equipment for GIS/LIS Applications
- Integration of Photogrammetric/Remote Sensing data with LIS and GIS Data Bases
- Merging of Multi-Source Data Sets
- Algorithms for the Rectification, Registration and Integration of Data Sets
- Computer Graphics for the Display of Integrated Data Sets
- Feature Extraction from Merged Data Sets
- National, State and Regional Applications

The intent of the Symposium is to bring together representatives of ISPRS along with colleagues from the International Cartographic Association (ICA), the Federation International des Geometres (FIG), and the ASPRS-ACSM who are interested in using photogrammetric and remote sensing data with LIS/GIS. Those wishing to present a paper should submit an abstract of approximately 200 words (in English) by September 20, 1986 to:

Dr. Roy Welch (Chairman, ISPRS Intercommission WG III/IV)
Laboratory for Remote Sensing and Mapping Science
Department of Geography
University of Georgia
Athens, GA 30602
USA